Transverse Acoustic Modes of Biogenic and α,ω-Polyamines: A Study by Inelastic Neutron Scattering and Raman Spectroscopies Coupled to DFT Calculations

Luís A. E. Batista de Carvalho,[†] **M. Paula M. Marques,**[*,†,‡] **and John Tomkinson**[§]

Research Unit "Molecular Physical-Chemistry", University of Coimbra, 3000 Coimbra, Portugal, Biochemistry Department, University of Coimbra, 3000 Coimbra, Portugal, and ISIS Facility, The Rutherford Appleton Laboratory, Chilton, United Kingdom

A complete analysis of the transverse acoustic modes (TAMs) for the homologous series of α,ω-diamines ($H_2N(CH_2)_nNH_2$) ($n = 2-10$, $n = 12$) as well as for the biogenic polyamines spermidine and spermine was undertaken, by Raman and inelastic neutron scattering (INS) spectroscopies combined with density functional theory (DFT) calculations. A complete assignment of the whole set of TAMs was carried out, for both the undeuterated and N-deuterated species. 1,2-Diaminoethane was found to display exceptional behavior, probably due to the formation of dimers in the solid state. An *n*-even/*n*-odd dependence of the low frequency INS pattern was observed for these polyamines. The very good accordance between their INS experimental TAMs and the ones previously reported for the corresponding *n*-alkanes suggest a close conformational similarity between these systems.

1. Introduction

Biogenic polyamines, present in almost all living organisms, are products of the decarboxylation of amino acids. Putrescine—1,4-diaminobutane, $H_2N(CH_2)_4NH_2$—is the first member in the polyamine pathway, biosynthesized from arginine and the precursor of spermidine ($H_2N(CH_2)_3NH(CH_2)_4NH_2$) and spermine ($H_2N(CH_2)_3NH(CH_2)_4NH(CH_2)_3NH_2$). Under physiological conditions, these linear amines are totally protonated and behave as natural polycations. They are known to be implicated in a bewildering number of cellular functions,[1−6] being essential for eukaryotic cell growth and differentiation, as well as for maintaining the native structure of several biological macromolecules while affecting the activity of others,[1,7] through tightly regulated concentration-dependent processes. The understanding of this vital biological role of polyamines requires a thorough knowledge of their structural preferences, which will hopefully allow an explanation of the biochemical mechanisms through which they act in living organisms.

This conformational behavior can be analyzed through vibrational spectroscopic methods coupled to theoretical calculations. Inelastic neutron scattering (INS) spectroscopy, in particular, is a well suited technique for the study of this kind of highly hydrogenated system, specifically for observing low frequency vibrational modes such as the transverse and longitudinal acoustic modes (TAMs and LAMs, respectively).

The full longitudinal acoustic mode INS spectrum of a linear alkane was first determined for *n*-octadecane,[8] and the whole set of LAMs were observed and assigned for the 5 to 25 *n*-alkanes,[9] as well as for the polyamines $H_2N(CH_2)_nNH_2$ (*n* = 2−10 and *n* = 12), spermidine and spermine.[10] The transverse vibrational modes of the *n*-alkanes pentane to dodecane were also reported.[11] These transverse acoustic-like vibrations (TAMs), associated to out-of-plane bending modes of the $-(CH_2-CH_2)_n-$ linear chain, are known to be only partially active in optical spectroscopy (both Raman and infrared) and to give rise to intense features in the INS spectra. They occur in the region below ~250 cm⁻¹, which also comprises the external (i.e., intermolecular) vibrational modes.

The present work is focused on the analysis of these low-lying transverse acoustic vibrational modes for the homologous series of α,ω-diamines ($H_2N(CH_2)_nNH_2$) (*n* = 2−10, *n* = 12), as well as for the biogenic polyamines spermidine and spermine (Figure 1). Vibrational spectroscopy, both Raman and INS, combined with density functional theory (DFT) calculations was used for studying the undeuterated and N-deuterated species. A complete assignment of the TAMs was carried out, following a previous study of the corresponding longitudinal modes (LAMs).[10]

2. Experimental Methods

2.1. INS Spectroscopy. The INS spectra were obtained in the Rutherford Appleton Laboratory (United Kingdom), at the ISIS pulsed neutron source, on the TOSCA spectrometer. This is an indirect geometry time-of-flight, high resolution (($\Delta E/E$) ~2%), broad range spectrometer.[12] Solid compounds (2−3 g) were wrapped in aluminum foil, while the liquids were placed in thin walled aluminum cans, which filled the beam. The samples were cooled to ~20 K before collecting the spectra. Data were recorded in the energy range from 16 to 4000 cm⁻¹ and converted to the conventional scattering law, $S(Q,\nu)$, versus energy tranfer (in cm⁻¹) through standard programs.

2.2. Raman Spectroscopy. The Raman spectra performed at room temperature were obtained on a Spex Ramalog 1403 double spectrometer (focal distance 0.85 m, aperture *f*/7.8) equipped with holographic gratings of 1800 grooves·mm⁻¹ and

* To whom correspondence should be addressed. Present address: Biochemistry Department, Faculty of Science and Technology, University of Coimbra, Apartado 3126, 3001-401 Coimbra, Portugal. Phone: +351 239854462. Fax: +351 239826541. E-mail: pmc@ci.uc.pt.
† Research Unit "Molecular Physical-Chemistry", University of Coimbra.
‡ Biochemistry Department, University of Coimbra.
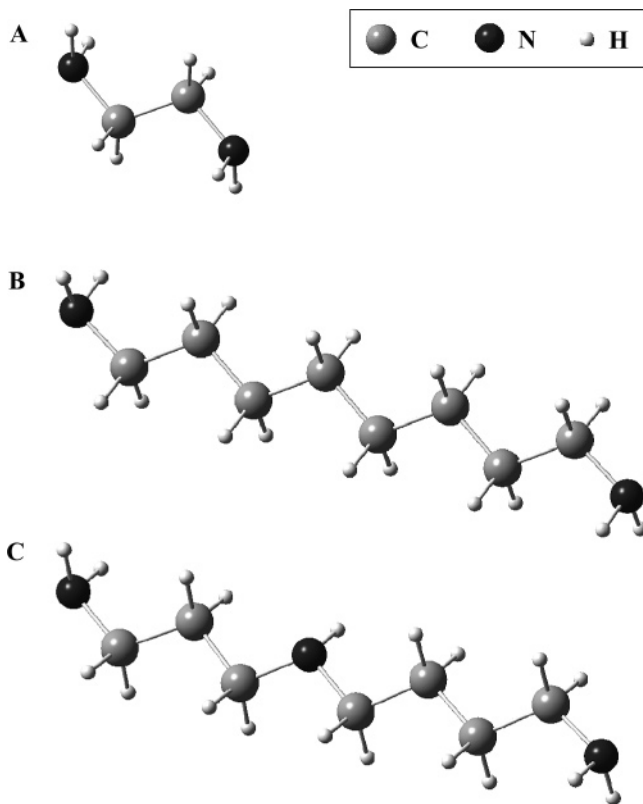§ The Rutherford Appleton Laboratory.

Figure 1. Calculated (B3LYP/6-31G*) all-trans conformations for some of the polyamines studied in this work: (A) 1,2-diaminoethane; (B) 1,8-diaminooctane; (C) spermidine.

a detector assembly containing a thermoelectrically cooled Hamamatsu R928 photomultiplier tube. The spectrometer operated with slits of 320 μm and 1 cm^{-1} s^{-1}. The 514.5 nm line of an Ar$^+$ laser (Coherent, model Innova 300) was used as excitation radiation, providing ~100 mW at the sample position.

Below room temperature (~220 K), a homemade Harney-Miller-type assembly was used, on a triple monochromator Jobin-Yvon T64000 Raman system (focal distance 0.640 m, aperture f/7.5) equipped with holographic gratings of 1800 grooves·mm^{-1}. The premonochromator stage was used in the subtractive mode. The detection system was a liquid nitrogen cooled nonintensified 578 × 385 pixel (1/2″) charge coupled device (CCD) chip. An Ar$^+$ laser (Coherent, model Innova 300-05) was used as the light source, the output of which at 514.5 nm was adjusted to provide between 60 and 80 mW at the sample position. A 90° geometry, between the incident radiation and the collecting system, was employed. The entrance slit was set to 200 μm, and the slit between the premonochromator and the spectrograph was opened to 12 mm.

Samples were sealed in Kimax glass capillary tubes of 0.8 mm inner diameter. Under the above-mentioned conditions, the error in wavenumbers was estimated to be within 1 cm^{-1}.

2.3. DFT Calculations. The quantum mechanical calculations—geometry optimization and calculation of the harmonic vibrational frequencies—were performed using the GAUSSIAN 98W program,[13] within the density functional theory (DFT) approach in order to properly represent the electron correlation effects (particularly important in this kind of nitrogen-containing system). The B3LYP hybrid method, which includes a mixture of HF and DFT exchange terms and the gradient-corrected correlation functional of Lee, Yang, and Parr[14,15] as proposed and parametrized by Becke,[16,17] was used, along with the double-ζ split valence basis set 6-31G*.[18]

Only the geometries with all skeletal dihedral angles equal to 180° (all-trans) were considered in the present work. Molecular geometries were fully optimized by the Berny algorithm, using redundant internal coordinates:[19] the bond lengths to within ~0.1 pm and the bond angles to within ~0.1°. The final root-mean-square (rms) gradients were always less than 3 × 10^{-4} hartree·b^{-1} or hartree·bohr^{-1}.

The calculated INS transition intensities were obtained using the a-CLIMAX program,[20] which calculates the INS spectrum corresponding to the results yielded by the quantum mechanical calculations. In this case, the vibrational mean square atomic displacements are the most important outputs.

2.4. Reagents. All of the polyamines were purchased from Sigma-Aldrich. The N-deuterated compounds were obtained by mixing the amines with D$_2$O (~10% excess) and distilling under vacuum (with this process being repeated at least three times). The solid amines were purified by sublimation, while the liquids were distilled under vacuum. With all of the samples being air or moisture sensitive, they were always handled in a glovebox under an argon atmosphere.

3. Results and Discussion

The conformational preferences of alkylamines are mainly determined by intra- versus intermolecular (N)H···:N and (C)H···:N hydrogen bonds, as previously confirmed by both quantum mechanical calculations and vibrational spectroscopy studies.[21-23] These molecules can adopt different geometries, by varying the dihedral angles that determine their overall orientation, the most common conformations having skeletal dihedral angles near 60° (gauche), 180° (trans), and −60° (gauche′). However, the crystal packing of the polyamines in the solid state—which corresponds to the present study—is compatible only to the all-trans conformers (Figure 1) that can be compared to saturated linear alkanes, for which the all-trans geometry has long been recognized as being energetically the most favored.[24] Under these conditions, the formation of intramolecular hydrogen bonds is hindered, and only three effects are relevant in determining conformation: electrostatic and steric forces and intermolecular R−N−H···NH$_2$−R interactions (namely, at the terminal NH$_2$ groups of the chain[25]), which are probably quite strong due to the linear geometry of the samples and the marked directional nature of these hydrogen bonds.[26-29] In fact, these hydrogen-type bonds are clearly evidenced by the shift to low frequencies observed for the Raman ν_{NH_2} bands when going from the pure liquid to the solid state.

DFT calculations were carried out for both the undeuterated and N-deuterated all-trans configurations of the series of amines (H$_2$N(CH$_2$)$_n$NH$_2$) ($n = 2-10$, $n = 12$), spermidine and spermine, in view of allowing a complete assignment of their low frequency vibrational spectra. No polarization functions were included in the hydrogen atoms, since it was verified, in previous studies on these systems,[10] that the 6-31G* basis set yields reliable results (in good accordance with the corresponding MP2/6-31G** data). The members of the H$_2$N(CH$_2$)$_n$NH$_2$ ($n = 2-10$, $n = 12$) series exhibit C_{2h} symmetry for $n =$ even and C_{2v} symmetry for $n =$ odd. Spermidine and spermine, in turn, were found to have a much lower symmetry, C_1 and C_2, respectively.

A complete assignment of the TAMs for the whole series of polyamines under study is comprised in Tables 1 (undeuterated amines) and 2 (N-deuterated amines). This was carried out in light of the DFT calculations performed for these systems and by comparison with analogous data obtained for the corresponding n-alkanes.[11] In accordance with the LAMs previously reported for the same amines,[10] all of the TAMs display the

TABLE 1: Transverse Acoustic Vibrational Modes (TAMs) for the $H_2N(CH_2)_nNH_2$ ($n = 2-10$, $n = 12$) Diamines, Spermidine and Spermine

N			i										
			1	2	3	4	5	6	7	8	9	10	11
4	1,2dae (C_{2h})	exptl (INS)	207										
		exptl (Ram)											
		calcd[a]	145 (A_u)										
		κ	0.500										
5	1,3dap (C_{2v})	exptl (INS)	191	180									
				174									
		av[b]		178									
		exptl (Ram)		180									
		calcd	125 (A_2)	120 (B_1)									
		κ	0.333	0.666									
6	1,4dab (C_{2h})	exptl (INS)	154	199	112								
			161	191									
		av[b]	158	195									
		exptl (Ram)	157	198									
		calcd	103 (A_u)	164 (B_g)	79 (A_u)								
		κ	0.250	0.500	0.750								
7	1,5dap (C_{2v})	exptl (INS)	134	202	167	111							
				189		103							
		av[b]		196		107							
		exptl (Ram)		183	177	108							
		calcd	89 (A_2)	162 (B_1)	150 (A_2)	68 (B_1)							
		κ	0.200	0.400	0.600	0.800							
8	1,6dah (C_{2h})	exptl (INS)	117	177	205	151	99						
			109	162	194								
		av[b]	113	170	200								
		exptl (Ram)				149							
		calcd	70 (A_u)	141 (B_g)	174 (A_u)	119 (B_g)	50 (A_u)						
		κ	0.167	0.333	0.500	0.667	0.833						
9	1,7dah (C_{2v})	exptl (INS)	137	164	199	187	152	119					
		av[b]											
		exptl (Ram)					148						
		calcd	73 (A_2)	129 (B_1)	173 (A_2)	163 (B_1)	103 (A_2)	46 (B_1)					
		κ	0.143	0.286	0.429	0.571	0.714	0.857					
10	1,8dao (C_{2h})	exptl (INS)	113	163	188	207	175	141	104				
					202	202							
		av[b]			195	205							
		exptl (Ram)	118					137					
		calcd	58 (A_u)	113 (B_g)	159 (A_u)	171 (B_g)	138 (A_u)	82 (B_g)	33 (A_u)				
		κ	0.125	0.250	0.375	0.500	0.625	0.750	0.875				
	spd (C_1)	exptl (INS)		166	198	211	183	146	110				
		av[b]											
		exptl (Ram)	131		197		181	149	111				
		calcd	66	116	165	179	138	85	35				
		κ	0.125	0.250	0.375	0.500	0.625	0.750	0.875				
11	1,9dan (C_{2v})	exptl (INS)	123	156	182	204	198	169	136	106			
		av[b]											
		exptl (Ram)	123			203			140				
		calcd	63 (A_2)	108 (B_1)	149 (A_2)	177 (B_1)	170 (A_2)	126 (B_1)	76 (A_2)	33 (B_1)			
		κ	0.111	0.222	0.333	0.444	0.556	0.667	0.778	0.889			
12	1,10dad (C_{2h})	exptl (INS)	123	148	170	201	206	180	157	137	107		
		av[b]											
		exptl (Ram)				201		176		132			
		calcd	56 (A_u)	98 (B_g)	139 (A_u)	173 (B_g)	180 (A_u)	153 (B_g)	109 (A_u)	63 (B_g)	28 (A_u)		
		κ	0.100	0.200	0.300	0.400	0.500	0.600	0.700	0.800	0.900		
14	1,12dad (C_{2h})	exptl (INS)	106	132	152	181	197	205	189	156	138	106	87
					148		205	197		152			
					150		201	201		154			
		av[b]											
		exptl (Ram)		127		175		197		152		109	
		calcd	43 (A_u)	80 (B_g)	117 (A_u)	149 (B_g)	172 (A_u)	172 (B_g)	156 (A_u)	121 (B_g)	80 (A_u)	43 (B_g)	18 (A_u)
		κ	0.083	0.167	0.250	0.333	0.417	0.500	0.583	0.667	0.750	0.833	0.917
	sp (C_1)	exptl (INS)	115	140	163	190	208	216	190	170	140	128	96
					170		197	208		163			
					167		203	212		167			
		av[b]											
		exptl (Ram)	112	140			200				140		
		calcd	46	86	122	157	174	183	157	122	86	54	21
		κ	0.083	0.167	0.250	0.333	0.417	0.500	0.583	0.667	0.750	0.833	0.917

[a] At the B3LYP/6-31G* level. $i = 1, 2, ... , (N - 3)$; $κ = i/(N - 2)$; N represents the number of beads in the chain, and k is the corresponding wavevector. [b] Mean value of the observed Davydov components.

same INS intensity. When comparing the experimental INS and Raman data (Figure 2), it is easily verified that while almost all of the TAMs are detected by INS, only some of these transverse modes are observed in the Raman spectra (Tables 1

TABLE 2: Transverse Acoustic Vibrational Modes (TAMs) for the $D_2N(CH_2)_nND_2$ ($n = 2-10$, $N = 12$) Diamines, Spermidine-N-d_5 and Spermine-N-d_6

			i										
N			1	2	3	4	5	6	7	8	9	10	11
4	1,2dae (C_{2h})	exptl (INS)											
		exptl (Ram)											
		calcd[a]	132 (A$_u$)										
		κ	0.500										
5	1,3dap (C_{2v})	exptl (INS) av[b]											
		exptl (Ram)											
		calcd	112 (A$_2$)	112 (B$_1$)									
		κ	0.333	0.666									
6	1,4dab (C_{2h})	exptl (INS) av[b]	150	189	106								
		exptl (Ram)	160		110								
		calcd	95 (A$_u$)	159 (B$_g$)	74 (A$_u$)								
		κ	0.250	0.500	0.750								
7	1,5dap (C_{2v})	exptl (INS) av[b]		183									
		exptl (Ram)			179								
		calcd	80 (A$_2$)	153 (B$_1$)	147 (A$_2$)	66 (B$_1$)							
		κ	0.200	0.400	0.600	0.800							
8	1,6dah (C_{2h})	exptl (INS)	115	178	203	152	104						
				173	194								
		av[b]		176	199								
		exptl (Ram)		176		147							
		calcd	64 (A$_u$)	134 (B$_g$)	171 (A$_u$)	116 (B$_g$)	48 (A$_u$)						
		κ	0.167	0.333	0.500	0.667	0.833						
9	1,7dah (C_{2v})	exptl (INS) av[b]	132	161	193	183	150						
		exptl (Ram)		161			146						
		calcd	66 (A$_2$)	122 (B$_1$)	168 (A$_2$)	160 (B$_1$)	101 (A$_2$)	45 (B$_1$)					
		κ	0.143	0.286	0.429	0.571	0.714	0.857					
10	1,8dao (C_{2h})	exptl (INS)	112	155	185	204	168	138	102				
					198	198							
		av[b]			192	201							
		exptl (Ram)	116	148			165	135					
		calcd	55 (A$_u$)	107 (B$_g$)	156 (A$_u$)	170 (B$_g$)	134 (A$_u$)	80 (B$_g$)	32 (A$_u$)				
		κ	0.125	0.250	0.375	0.500	0.625	0.750	0.875				
	spd (C_1)	exptl (INS) av[b]		163	190	205	175	143	108				
		exptl (Ram)	130		190		177	148	110				
		calcd	61	108	159	174	134	83	33				
		κ	0.125	0.250	0.375	0.500	0.625	0.750	0.875				
11	1,9dan (C_{2v})	exptl (INS) av[b]		154	185	201	196	168	135	104			
		exptl (Ram)	120				199			105			
		calcd	58 (A$_2$)	102 (B$_1$)	144 (A$_2$)	175 (B$_1$)	169 (A$_2$)	124 (B$_1$)	73 (A$_2$)	33 (B$_1$)			
		κ	0.111	0.222	0.333	0.444	0.556	0.667	0.778	0.889			
12	1,10dad (C_{2h})	exptl (INS) av[b]	120	143	164	198	203	177	152	135	107		
		exptl (Ram)				197		173		132			
		calcd	53 (A$_u$)	94 (B$_g$)	134 (A$_u$)	170 (B$_g$)	177 (A$_u$)	151 (B$_g$)	108 (A$_u$)	62 (B$_g$)	27 (A$_u$)		
		κ	0.100	0.200	0.300	0.400	0.500	0.600	0.700	0.800	0.900		
14	1,12dad (C_{2h})	exptl (INS) av[b]	106	131	145	181	202	206	186	150	134	106	85
		exptl (Ram)		131		173				149		109	
		calcd	40 (A$_u$)	76 (B$_g$)	113 (A$_u$)	146 (B$_g$)	171 (A$_u$)	171 (B$_g$)	155 (A$_u$)	119 (B$_g$)	76 (A$_u$)	44 (B$_g$)	18 (A$_u$)
		κ	0.083	0.167	0.250	0.333	0.417	0.500	0.583	0.667	0.750	0.833	0.917
	sp (C_1)	exptl (INS)	114	138	158	181	192	206	185	168	138	125	95
						185	206		181				
		av[b]				183	199		183				
		exptl (Ram)	111	132	156	179	190		179		132		
		calcd	45	82	113	151	172	178	151	122	84	50	20
		κ	0.083	0.167	0.250	0.333	0.417	0.500	0.583	0.667	0.750	0.833	0.917

[a] At the B3LYP/6-31G* level. $i = 1, 2, \ldots, (N - 3)$; $\kappa = i/(N - 2)$; N represents the number of beads in the chain, and k is the corresponding wavevector. [b] Mean value of the observed Davydov components.

and 2). In fact, some of the TAMs are either very weak or symmetry forbidden transitions in Raman spectroscopy. Nevertheless, these optical selection rules were not always obeyed (e.g., 1,4-diaminobutane, Tables 1 and 2), which can be

explained by the significant mixing of these transverse vibrations with external modes (as discussed later). Deuteration of the samples led to the anticipated shifts to lower frequencies in both Raman and INS (Figure 3), as a result of the variations in both
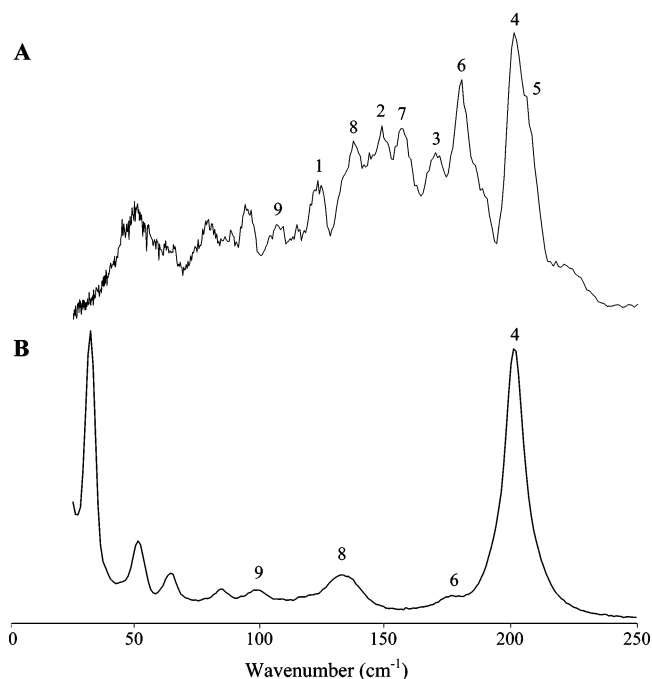
TAMs of Biogenic and α,ω-Polyamines

J. Phys. Chem. A, Vol. 110, No. 47, 2006 **12951**

Figure 2. Experimental INS (A) and Raman (B) spectra (16−250 cm⁻¹) for 1,10-diaminodecane. (The numbers refer to the corresponding TAM modes.)
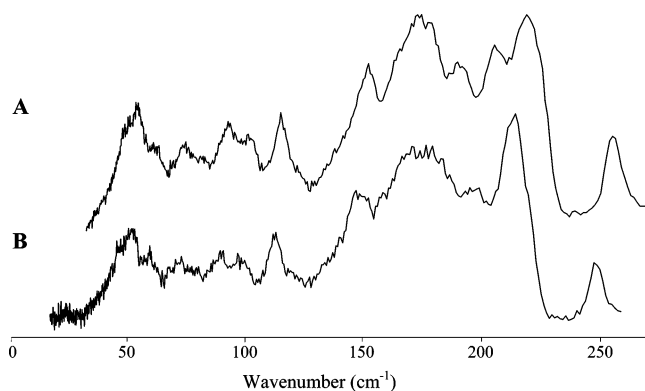

Figure 3. Experimental INS spectra (16−260 cm⁻¹, at 20 K) for spermidine, in its undeuterated (A) and N-deuterated (B) forms.

mass (frequencies) and scattering cross section (INS intensities). This shift was found to be about 2−3 cm⁻¹ for the TAM modes (Tables 1 and 2).

The transverse acoustic modes observed for the aliphatic amines studied here are directly related to their torsional vibrations, with each pair of carbons along the chain giving rise to an internal torsional coordinate, yielding a total of $N − 3$ TAMs (Tables 1 and 2). These low frequency bands are prone to intermolecular interactions and are thus dependent on the molecular packing in the condensed phase. This explains why there are more transverse modes observed experimentally then predicted theoretically. Davydov splitting was detected for many of the TAMs in the INS spectra, probably due to the occurrence of distinct solid state phases as a result of the rapid cooling to the low temperatures used in INS, leading to two crystallographically and energetically inequivalent conformations. This doubling of the unit cell was previously observed for n-alkanes[11] and extensively discussed for the particular case of n-octane,[30] for which spectral evidence of a low temperature (∼50 K) phase transition was reported, suggesting that this may be common to all n-alkanes as well as to the structurally similar linear amines presently studied.

Furthermore, the presence of several molecules in a crystal (or a packed solid state) generates an external force field, which is responsible for new vibrational modes, the so-called external modes (we locate these below ∼120 cm⁻¹ for the polyamines, as opposed to 80 cm⁻¹ for the n-alkanes[11]). Those external modes, of appropriate character, mix with the TAMs, and the closer they are in frequency, the larger the extent of mixing. Thus, the lower frequency TAMs are more affected by this mixing process, while the high frequency ones (those with intermediate κ values, see later) are less affected. As a result of this mode mixing, the experimental TAMs are pushed to higher wavenumbers than the external modes. We identify the gap detected around 120 cm⁻¹ in the INS pattern of the polyamines, and in the large number of bands observed between ∼120 and 210 cm⁻¹ (Figure 4), with that expected between the internal and external modes. The fact that the external mode region is extended to higher frequencies for the linear amines than the n-alkanes is mainly due to the occurrence of intermolecular R−HN−H···:NH₂−R contacts.

While the density of states corresponding to the external modes is not comprised of individual transitions, the observed TAMs remain sharp features. Although the impact of this mixing is more obvious for the TAM modes, similar effects were reported for some of the LAMs in these systems,[10] namely, for the lowest frequency LAM1 of the longest amines. Also, a slight TAM−LAM coupling may be detected for wavenumbers near 200 cm⁻¹; in fact, the LAM1 frequency was found to tend to the value of the presently reported TAM_max (∼209 cm⁻¹, Tables 1 and 2) upon lengthening of the chain.[10]

A very good agreement was found between the INS experimental TAMs presently observed and the low frequency neutron scattering pattern of the corresponding n-alkanes[11] (Figure 5), which corroborates the idea of a significant conformational similarity (in the solid state) between these two sets of compounds. While the vibrational pattern of the n-alkanes comprises CH₃ torsions (τ_{CH_3}) as isolated and intense features around 250 cm⁻¹, in the linear amines presently investigated, the torsional modes of the terminal NH₂ groups (τ_{NH_2}) are not clearly observed by INS above 210 cm⁻¹, as would be expected from the theoretical calculations. This suggests the occurrence of R−N−H···NH₂−R intermolecular interactions, as previously discussed.[10] Actually, the vibrational consequences of the intermolecular hydrogen bonds occurring in this kind of system cannot be predicted by the isolated molecule approach used in the calculations presently carried out, that consider only internal forces. Therefore, some discrepancies between calculated and experimental data are to be expected for the oscillators involved in intermolecular close contacts. Moreover, the result of the overlay between the external and internal modes is not accounted for in this theoretical treatment, which explains the significant differences between the experimental and predicted lowest TAM values (Tables 1 and 2).

In the low frequency region presently analyzed, 1,2-diaminoethane, the shortest element of the series, was found to display exceptional behavior, similarly to what was previously reported for its LAM modes.[10] This is proposed to be due to the occurrence of dimers in the solid state for this small molecule, upon formation of intermolecular H₂N···H interactions: H₂N(CH₂)₂-NH₂···NH₂(CH₂)₂NH₂ (comprising eight beads). Actually, the INS low frequency pattern observed for 1,2-diaminoethane displays a reasonable accord with that of 1,6-diaminohexane ($n = 8$) (Figure 4).

Figure 6 displays the plots of the INS band center positions of the experimental TAMs observed for the undeuterated and
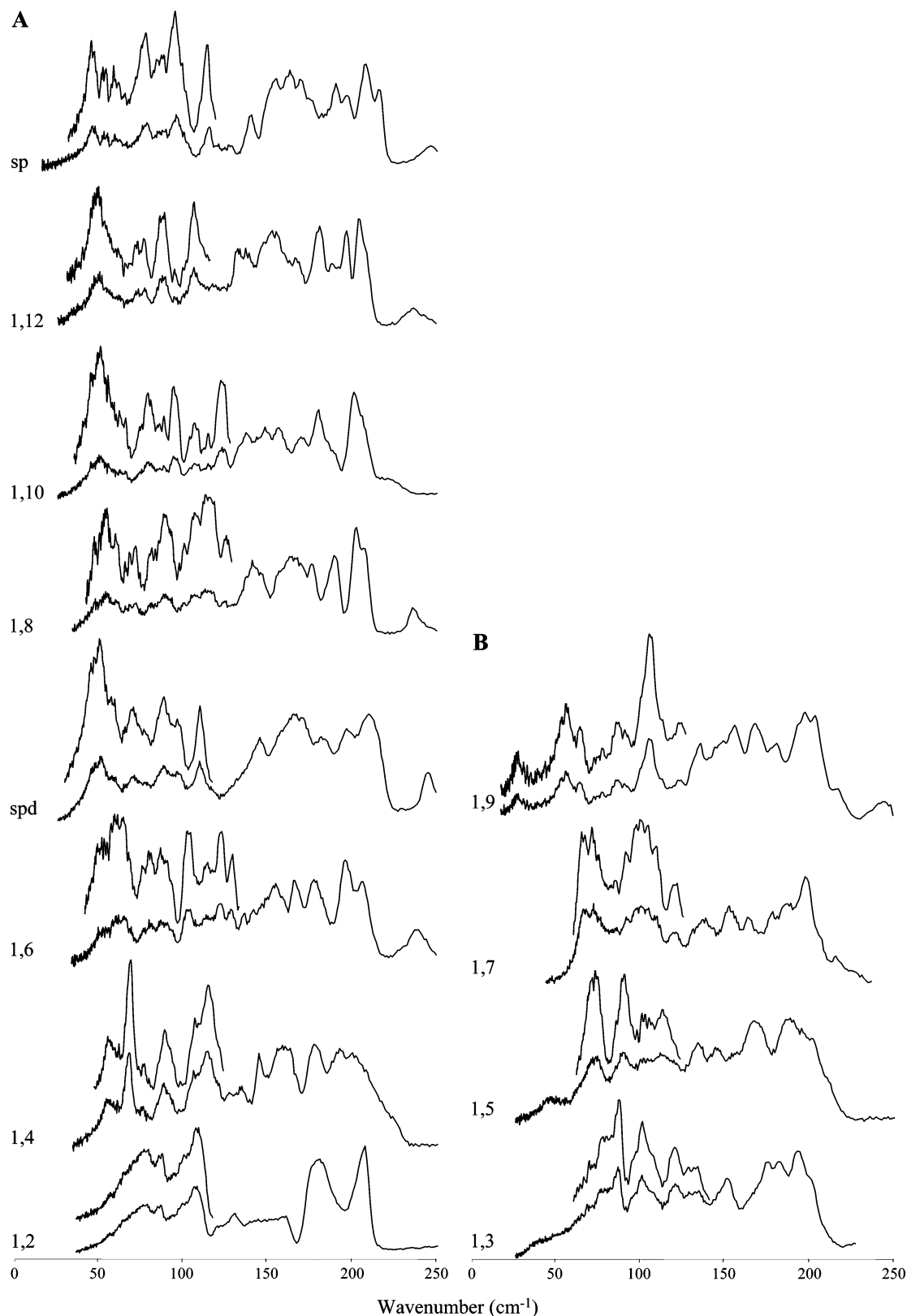
Figure 4. Experimental INS spectra (16−250 cm^{-1}, at 20 K) for the series of polyamines studied: (A) n = even; (B) n = odd. (The following abreviations were used: 1,n = 1,2- to 1,12-H$_2$N(CH$_2$)$_n$NH$_2$ (n = 2−12); spd, spermidine; sp, spermine.)

deuterated amines, as a function of their ideal wavevectors (κ). The upper frequency band-heads ((ν_{TAM})$_{max}$) were observed at ~212 cm^{-1} for the undeuterated molecules (Figure 6A) and at 206 cm^{-1} for the N-deuterated ones (Figure 6B). (ν_{TAM})$_{max}$ was found to display a steady increase as the amine chain lengthens, from 1,2-diaminoethane to 1,12-diaminododecane and spermine.

Moreover, the value of the ideal wavevectors (κ) corresponding to a maximum TAM frequency, κ_{max}, estimated to be 0.5 for both the undeuterated and N-deuterated amines, remained nearly constant across the series. This is in accordance with what was previously verified for the LAM behavior of these same amines,[10] as well as for the TAMs and LAMs of *n*-alkanes.[9,11]
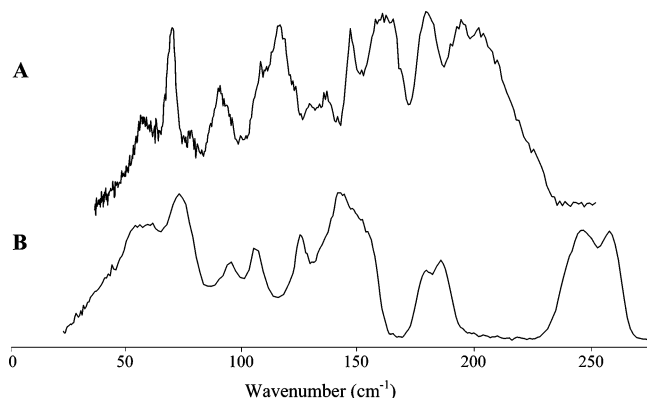
TAMs of Biogenic and α,ω-Polyamines

J. Phys. Chem. A, Vol. 110, No. 47, 2006 **12953**

Figure 5. Experimental INS spectra (16−275 cm^{-1}, at 20 K) for 1,4-diaminobutane (A) and *n*-hexane (from ref 11) (B).
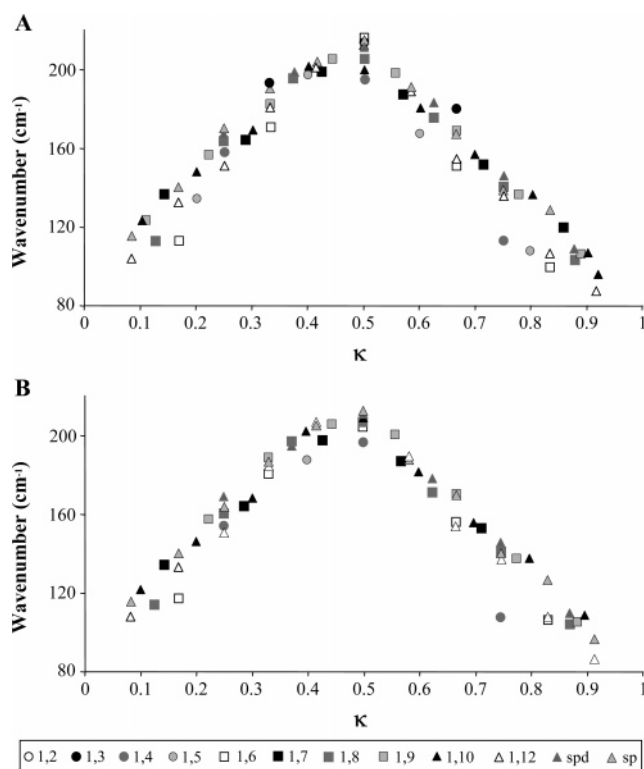

Figure 6. Plot of the INS band center positions (cm^{-1}) for the TAMs observed for the series of polyamines studied, as a function of their ideal wavevectors (κ): (A) undeuterated amines; (B) N-deuterated amines. (TAM$_{max}$ ∼200 cm^{-1}. The effects of Davydov splitting were averaged out. The following abreviations were used: 1,*n* = 1,2- to 1,12-H$_2$N(CH$_2$)$_n$NH$_2$ (*n* = 2−12); spd, spermidine; sp, spermine).

Since the observed κ_{max} did not deviate from the model value of 0.5, it is suggested that the dynamic coupling of the chain torsional modes with the higher frequency CH$_2$ rocking vibrations (between ∼800 and 1250 cm^{-1}) is not significant in these systems.

An *n*-even/*n*-odd dependence of the low frequency INS vibrational spectra was found for the series of polyamines studied, in agreement with the reported results for their vibrational data in the region above 250 cm^{-1},[10] and also with the variations found for a homologous series of *n*-alkanes (*n* = 5−25).[8,9,11] This *n*-odd/*n*-even alternation of physical properties and INS pattern should be related to a distinct packing arrangement of the linear amines, which is expected to be tighter for even-membered molecules and less dense for *n* = odd, similarly to that was previously recognized for *n*-alkanes.[31,32]

Therefore, the TAM dispersion curves for the two sets of polyamines display only subtle differences.

4. Conclusions

The use of the complementary INS and Raman spectroscopic techniques, coupled to DFT calculations, allowed the complete assignment of the TAM modes for the series of linear aliphatic amines H$_2$N(CH$_2$)$_n$NH$_2$ (*n* = 2−10, *n* = 12), spermidine and spermine, both in their undeuterated and N-deuterated forms. The quantum mechanical calculations, performed at the B3LYP/6-31G* level for the all-trans conformations of the polyamines, were showed to adequately mimic these kinds of linear nitrogen-containing molecules.

An *n*-even/*n*-odd dependence of the low frequency neutron scattering pattern was observed, probably as the result of a distinct packing arrangement of the amines in the condensed phase, namely, the tighter packing of the even-membered chains relative to the odd-membered ones (as previously reported for *n*-alkanes[11]).

The conformational similarity (in the solid state) between the linear aliphatic polyamines studied in this work and the analogous *n*-alkanes justifies the remarkably good accordance between the corresponding INS experimental TAMs (similarly to what was previously reported for the LAM modes[8−10]).

The present study, coupled to the previously reported work on the same polyamine series,[10] has allowed the achievement of a complete and reliable assignment of all the low energy modes of these systems, both tranverse and longitudinal. Knowledge of the conformational behavior of linear polyamines, strongly determined by intermolecular R−HN−H···NH$_2$−R hydrogen-type interactions mainly ocurring in condensed phases, may thus help one to better understand the diverse and often vital biological role of these kinds of molecules (namely, in cell growth and differentiation processes and in cancer prevention and therapy).

References and Notes

(1) Tabor, C. W.; Tabor, H. *Annu. Rev. Biochem.* **1984**, *53* 749 and references therein.

(2) Auvinen, M.; Passinen, A.; Anderson, L. C.; Holtta, E. *Nature (London)* **1992**, *360*, 355.

(3) O'Brien, T. G.; Megosh, L. C.; Gilliard, G.; Soler, A. P. *Cancer Res.* **1997**, *57*, 2630 and references therein.

(4) Xie, X.; Gillies, R. J.; Gerner, E. W. *J. Biol. Chem.* **1997**, *272*, 20484.

(5) Vassileva, V.; Ignatov, G. *Bulg. J. Plant Physiol.* **1999**, *25*, 49.

(6) Guo, D.; Lu, Z. *J. Gen. Physiol.* **2000**, *115*, 783.

(7) Medina, M. A.; Urdiales, J. L.; Rodriguez-Caso, C.; Ramírez, F. J.; Sánchez-Juménez, F. *Crit. Rev. Biochem. Mol. Biol.* **2003**, *38*, 23.

(8) Parker, S. F.; Braden, D. A.; Tomkinson, J.; Hudson, B. S. *J. Phys. Chem. B* **1998**, *102*, 5955.

(9) Braden, D. A.; Parker, S. F.; Tomkinson, J.; Hudson, B. S. *J. Chem. Phys.* **1999**, *111*, 429.

(10) Marques, M. P. M.; Batista de Carvalho, L. A. E.; Tomkinson, J. *J. Phys. Chem. A* **2002**, *106*, 2473.

(11) Tomkinson, J.; D. A.; Parker, S. F.; Braden, D. A.; Hudson, B. S. *Phys. Chem. Chem. Phys.* **2002**, *4*, 716.

(12) www.isis.rl.ac.uk.

(13) Frisch, M. J.; et al. *Gaussian 98*, revision A.9; Gaussian Inc.: Pittsburgh, PA, 1998.

(14) Lee, C.; Yang, W.; Parr, R. G. *Phys. Rev.* **1988**, *B37*, 785.

(15) Miehlich, B.; Savin, A.; Stoll, H.; Preuss, H. *Chem. Phys. Lett.* **1989**, *157*, 200.

(16) Becke, A. D. *Phys. Rev.* **1988**, *A38*, 3098.

(17) Becke, A. D. *J. Chem. Phys.* **1993**, *98*, 5648.

(18) Hariharan, P. C.; Pople, J. A. *Theor. Chim. Acta* **1973**, *28*, 213.

(19) Peng, C.; Ayala, P. Y.; Schlegel, H. B.; Frisch, M. J. *J. Comput. Chem.* **1996**, *17*, 49.

(20) Ramirez-Cuesta, A. J. *Comput. Phys. Commun.* **2004**, *157* (3), 226.

(21) Batista de Carvalho, L. A. E.; Amorim da Costa, A. M.; Teixeira-Dias, J. J. C. *THEOCHEM* **1990**, *205*, 327.

(22) Batista de Carvalho, L. A. E.; Lourenço, L. E.; Marques, M. P. M. *J. Mol. Struct.* **1999**, *482−483*, 639 and references therein.

(23) Marques, M. P. M.; Batista de Carvalho, L. A. E. In *COST 917: Biogenically Active Amines in Food*; Morgan, D. M. L., White, A., Sánchez-Jiménez, F., Bardocz, S., Eds.; European Comission: Luxemburg, 2000; Vol. IV, p 122.

(24) Mirkin, N. G.; Krimm, S. *J. Phys. Chem.* **1993**, *97*, 13887 and references therein.

(25) Giglio, E.; Liquori, A. M.; Puliti, R.; Ripamonti, A. *Acta Crystallogr.* **1966**, *20*, 652; 683.

(26) Taylor, R.; Kennard, O. *J. Am. Chem. Soc.* **1982**, *104*, 5063.

(27) Steiner, T. *Chem. Commun.* **1997**, 727.

(28) Katrusiak, A. *J. Mol. Struct.* **1999**, *474*, 125.

(29) Desiraju, G. R.; Steiner, T. The Weak Hydrogen Bond in Structural Chemistry and Biology. *IUCr Monographs on Chystallography−9*; Oxford University Press: Oxford, U.K., 1999; see also references therein.

(30) Neumann, M. A.; Johnson, M. R.; Radaelli, P. G. *Chem. Phys.* **2001**, *266*, 53.

(31) Mathisen, H.; Norman, N.; Pedersen, B. F. *Acta Chim. Scand.* **1967**, *21*, 127.

(32) Barnes, J.; Franconi, B. *J. Phys. Chem. Ref. Data* **1978**, *7*, 1309 and references therein.